

COMMUNICATION

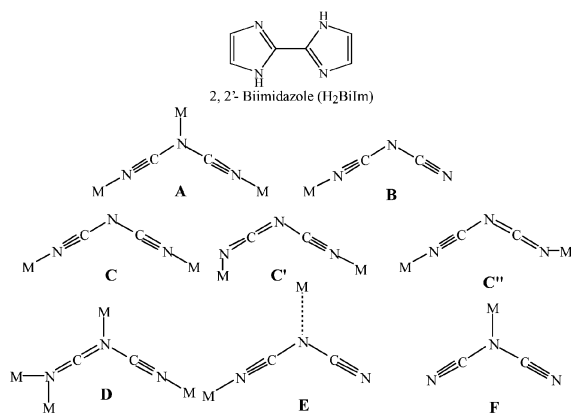
ChemComm
www.rsc.org/chemcommNovel coordination of dicyanamide, $[\text{N}(\text{CN})_2]^-$: preferential binding of the amide nitrogenShireen R. Marshall,^a Christopher D. Incarvito,^b William W. Shum,^a Arnold L. Rheingold^b and Joel S. Miller^{*a}^a Department of Chemistry, University of Utah, 315 S. 1400 E. RM 2124, Salt Lake City, UT 84112-0850, USA. E-mail: jmiller@chem.utah.edu^b Department of Chemistry, University of Delaware, Newark, DE 19716, USA. E-mail: arnrhein@udel.edu

Received (in Purdue, West Lafayette, IN, USA) 10th September 2002, Accepted 20th September 2002

First published as an Advance Article on the web 6th November 2002

$\text{Co}^{\text{II}}[\text{N}(\text{CN})_2]_2(\text{H}_2\text{BiIm})_2$, **1**, and $\{\text{Co}^{\text{II}}[\text{N}(\text{CN})_2](\text{H}_2\text{BiIm})_2\text{Cl}\}$, **2** (H_2BiIm = 2,2'-biimidazole) have been structurally, spectroscopically, and magnetically characterized with both containing dicyanamides bound in unprecedented manners; namely, solely *via* the amide nitrogen for **1**, and *via* an imide N forming 1-D helical chains for **2**.

Dicyanamide has been used for molecule-based magnets as well as extended network structures. Homoleptic $\text{M}^{\text{II}}[\text{N}(\text{CN})_2]_2$ and heteroleptic systems, $\text{M}^{\text{II}}[\text{N}(\text{CN})_2]_2\text{L}_x$ have been investigated. Materials with μ_3 - $[\text{N}(\text{CN})_2]^-$ bridging (**A**) stabilize ferro- or weak ferromagnetic ordering, while $\mu_{1,5}$ -bridging (**C**) propagates weak antiferromagnetic coupling. The systems studied have modes **A–E** (**A**: homoleptic systems, **B** and **C**: heteroleptic systems, **D**: $\text{Me}_2\text{Ti}[\text{N}(\text{CN})_2]_2$ and **E**²). Heretofore, bonding *via* the amide N (**F**) has been elusive, but is reported herein in $\text{Co}^{\text{II}}[\text{N}(\text{CN})_2]_2(\text{H}_2\text{BiIm})_2$ (H_2BiIm = 2,2'-biimidazole). $\{\text{Co}^{\text{II}}[\text{N}(\text{CN})_2](\text{H}_2\text{BiIm})_2\text{Cl}\}$, **2**, displays a rare helical chain propagated through $\mu_{1,5}$ -dicyanamide and imide bonding, **C'** and **C''**.



1 was made by adding 2 equiv. of H_2BiIm ³ to a hot aqueous solution of $\text{CoCl}_2 \cdot 6\text{H}_2\text{O}$, which forms $\text{CoCl}_2(\text{H}_2\text{BiIm})_2$ *in situ*,⁴ after which 2 equiv. of solid $\text{Na}[\text{N}(\text{CN})_2]$ were added. After filtering and slow evaporation at room temperature for two weeks, light orange block crystals were filtered and washed with water.† **2** was synthesized in a similar manner using a 1:1:1 stoichiometric mixture of the reagents. Dark orange needles were obtained following several weeks of slow evaporation.†

1 is composed of octahedral Co^{II} coordinated to six nitrogens. The equatorial positions are occupied by two bidentate H_2BiIm molecules, while the axial positions are coordinated by amide nitrogens from two dicyanamides (Fig. 1). The $\text{Co}-\text{N}_{\text{amide}}$ distance [2.1912(13) Å] is slightly elongated relative to μ_3 -bound $\alpha\text{-Co}[\text{N}(\text{CN})_2]_2$ [2.161(2) Å].⁵ Preferential binding of the amide rather than the nitrile nitrogen of dicyanamide is unprecedented, as the nitrile nitrogens are more electronegative, have greater electron delocalization, and can π -backbond. It is possible that electron donation from the H_2BiIm , in the preformed $\text{CoCl}_2(\text{H}_2\text{BiIm})_2$,⁴ creates a Co^{II} with an affinity for

the softer amide nitrogen of the dicyanamide ligand. This is evident for $\mu_{1,3}$ - $[\text{N}(\text{CN})_2]^-$ reported for $\beta\text{-Cu}[\text{N}(\text{CN})_2]_2(\text{imidazole})_6$ and $\text{Cu}(\text{bpca})(\text{H}_2\text{O})[\text{N}(\text{CN})_2]_2$ [bpca = bis(2-pyridylcarbonyl)amidate]. In these examples, however, the impetus for amide binding is ambiguous. The crystal structure of the latter reveals strong coordination through a nitrile nitrogen [$\text{Cu}-\text{N}_{\text{nitrile}}$ 1.962(2) Å] with simple electron donation from the amide nitrogen to the neighboring copper center [$\text{Cu}\cdots\text{N}_{\text{amide}}$ 2.7992(2) Å] so that crystal packing may drive the coordination.

1 is hydrogen bonded through the H atoms of H_2BiIm and the nitrile N's on neighboring molecules [H(4)–N(7) 2.016(2), H(2)–N(7) 2.487(2) Å]. This secondary network structure appears as zigzag chains running parallel to the *c*-axis (Fig. 2). Perpendicular to *c*, the zigzag chains form columns. The $\text{Co}\cdots\text{Co}$ separations are 7.162 (*a*), 7.684 (*b*) and 9.142 Å (*c*).

The IR of **1** shows strong absorptions at 2278, 2253, 2222, 2163 and 2140 cm^{-1} assigned to $\nu_{\text{C}\equiv\text{N}}$ of the dicyanamide ligand. These stretching frequencies resemble those observed for monodentate coordination (*e.g.* $\text{Na}[\text{N}(\text{CN})_2]$: 2288, 2236, 2228, 2181 cm^{-1}). However, the absorption at 2140 cm^{-1} , absent for monodentate coordination, is only slightly higher than the lowest energy absorption of unbound dicyanamide (*e.g.*, $[\text{PPh}_4][\text{N}(\text{CN})_2]$: 2227, 2188, 2130 cm^{-1}); consistent with

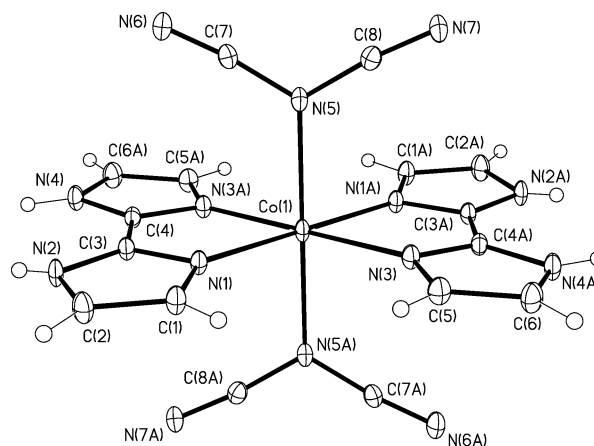


Fig. 1 ORTEP (30%) atom labeling scheme of **1**. Selected bond lengths (Å) and angles (°): $\text{Co}(1)-\text{N}(1)$ 2.1435(12), $\text{Co}(1)-\text{N}(3)$ 2.1268(12), $\text{Co}(1)-\text{N}(5)$ 2.1912(13), $\text{N}(5)-\text{C}(7)$ 1.3307(18), $\text{N}(5)-\text{C}(8)$ 1.3143(19), $\text{N}(6)-\text{C}(7)$ 1.154(2), $\text{N}(7)-\text{C}(8)$ 1.156(2), $\text{C}(1)-\text{C}(2)$ 1.364(2); $\text{N}(3)-\text{Co}(1)-\text{N}(1)$ 101.21(5), $\text{N}(3)-\text{Co}(1)-\text{N}(1)\#1$ 78.79(5), $\text{C}(8)-\text{N}(5)-\text{C}(7)$ 119.27(13), $\text{C}(8)-\text{N}(5)-\text{Co}(1)$ 118.72(10), $\text{C}(7)-\text{N}(5)-\text{Co}(1)$ 120.47(10).

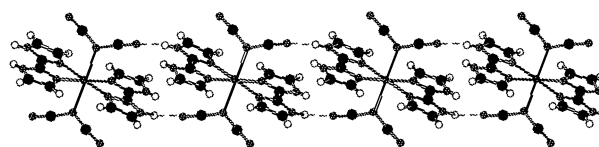


Fig. 2 Schematic showing the zigzag chain formed by hydrogen bonding [H(4)–N(7) 2.016 Å] in **1**.

DOI: 10.1039/b208872j

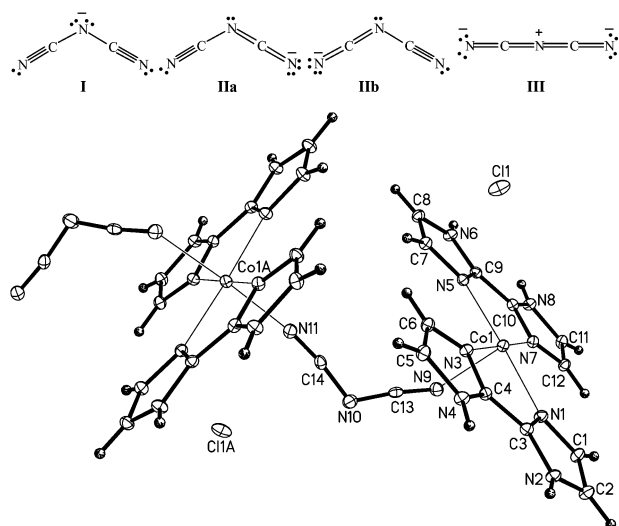


Fig. 3 ORTEP (30%) atom labeling scheme of **2**. Selected bond lengths (Å) and angles (°): Co(1)–N(1) 2.1386(18), Co(1)–N(3) 2.1593(18), Co(1)–N(5) 2.1372(18), Co(1)–N(7) 2.1325(18), Co(1)–N(9) 2.1900(19), Co(1)–N(11)#1 2.1133(19), N(9)–C(13) 1.162(3), C(13)–N(10) 1.299(3), C(14)–N(10) 1.311(3), C(14)–N(11) 1.155(3); C(13)–N(10)–C(14) 120.4(2), N(10)–C(14)–N(11) 173.0(2), N(1)–Co(1)–N(3) 78.72(7), N(5)–Co(1)–N(7) 79.09(7).

coordination through the amide nitrogen, which results in decreased electron density at the cyano groups. It is also important that the highest frequency is significantly less than 2300 cm^{-1} , which rules out the bidentate bridging and tridentate modes of attachment for dicyanamide.⁷ The ν_{CN} for **2** are observed at 2291, 2237 and 2162 cm^{-1} .

The Co^{II} of **2** is octahedrally coordinated to six nitrogens (Fig. 3). Four of which originate from two H_2BiIm ligands occupying equatorial sites. The two apical nitrogens are the nitrile ends of bridging $\mu_{1,5}$ -dicyanamides. Bridging through a single $\mu_{1,5}$ -dicyanamide leads to the formation of helical chains (Fig. 4),⁸ with the biimidazole planes of neighboring metal centers oriented perpendicular to one another, with nearest intra- and interchain metal–metal distances of 7.286 and 7.969 Å, respectively. Chloride ions are nestled in the pockets formed by the helices. The $\text{C}\equiv\text{N}-\text{Co}$ angles are 124.34(16) and 172.32(17)°, suggesting an abnormally large contribution from resonance structures **IIa** and **IIb**. The predominance of resonance structures **IIa** and **IIb** most likely results from an electrostatic interaction between the amide nitrogen and chloride [N...Cl 3.530(19) Å] (Fig. 4), which forces the negative charge to reside on the terminal (imide) nitrogen.

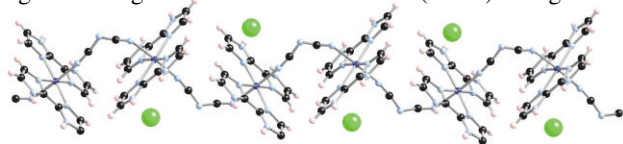


Fig. 4 Helical chain of $\{\text{Co}[\text{N}(\text{CN})_2](\text{H}_2\text{BiIm})_2\}\text{Cl}$, **2**.

The reciprocal magnetic susceptibilities, χ^{-1} , and χT products between 2 and 300 K are shown in Fig. 5. The observed room temperature χT values of 2.55 for **1** and 2.34 emu K mol^{-1} for **2** are consistent with $g = 2.33$ (2.54 emu K mol^{-1} , 4.51 μ_{B} expected) for **1** and $g = 2.22$ (2.31 emu K mol^{-1} expected) for **2**. $\chi T(T)$ could not be fit to the Curie–Weiss expression, but was fit to an expression that accounted for zero-field splitting D , eqn. (1) and intermolecular interactions, zJ , eqn. (2):⁹

$$\chi_{\text{zfs}} = \frac{Ng^2\mu_{\text{B}}^2}{k_{\text{B}}T} \left[\frac{1}{3} \frac{1+9e^{-2x}}{4(1+e^{-2x})} + \frac{2}{3} \frac{1+\frac{3k_{\text{B}}T}{4D}(1-e^{-2x})}{1+e^{-2x}} \right] + \text{TIP} \quad (1)$$

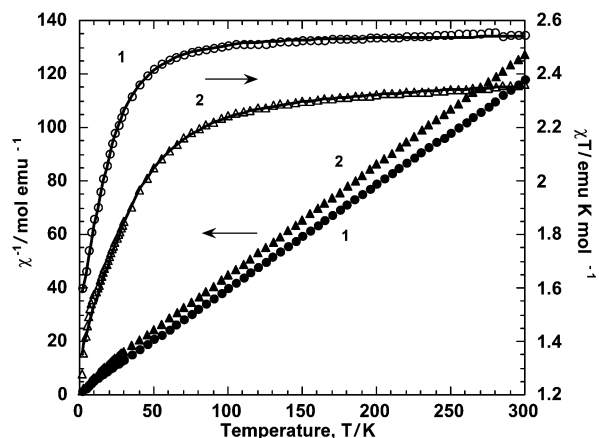


Fig. 5 Temperature dependence of χ^{-1} (●, ▲) and χT (○, △) for **1** and **2**, respectively. Solid lines are fits to eqn. (2).

$$\chi = \frac{\chi_{\text{zfs}}}{1 - \frac{2zJ\chi_{\text{zfs}}}{Ng^2\mu_{\text{B}}^2}} \quad (2)$$

where $x = D/k_{\text{B}}T$. The parameters obtained from the fit were $g = 2.33$ and $D = 23.3 \text{ cm}^{-1}$ for **1**, and $g = 2.22$, $D = 40.3 \text{ cm}^{-1}$, $zJ/k_{\text{B}} = -0.05 \text{ cm}^{-1}$, and $\text{TIP} = 170 \times 10^{-6} \text{ emu mol}^{-1}$ for **2**. The D values are in good agreement with previously reported values for octahedral Co^{II} of 32.5¹⁰ and 38.9 cm^{-1} .⁸ The decrease in χT below ~ 60 K for both **1** and **2** is the result of splitting of the ground state ${}^4\text{T}_{1\text{g}}$ levels that leads to a pseudo $S' = 1/2$ state. Additionally, very weak antiferromagnetic interactions ($zJ/k_{\text{B}} = -0.05 \text{ cm}^{-1}$) occur below 10 K for **2**.

The authors gratefully acknowledge the ACS-PRF (PRF No. 36165-AC5) and the U.S. Department of Energy (Grant No. DE-FG03-93ER45504) for support of this work.

Notes and references

† Crystal data for **1**: triclinic, $P\bar{1}$, $a = 7.1616(10)$, $b = 7.6838(10)$, $c = 9.1417(12)$ Å, $\alpha = 97.338(2)$, $\beta = 108.909(2)$, $\gamma = 94.916(2)^\circ$, $Z = 1$, $M = 459.33$, $U = 467.66(11)$ Å³, $D_{\text{c}} = 1.631 \text{ Mg m}^{-3}$, $T = 150(2)$ K, 5310 reflections collected, 2140 independent [$R(\text{int}) = 0.0186$], $R_1 = 0.0299$, $wR_2 = 0.1061$. CCDC 193518.

Crystal Data for **2**: monoclinic, $P2_1$, $a = 7.9690(5)$, $b = 13.8284(9)$, $c = 8.1547(5)$ Å, $\alpha = 110.5790(10)^\circ$, $Z = 2$, $M = 428.73$, $U = 841.29(9)$ Å³, $D = 1.692 \text{ Mg m}^{-3}$, $T = 150(2)$ K, 5359 reflections collected, 3644 independent [$R(\text{int}) = 0.0162$], $R_1 = 0.0268$, $wR_2 = 0.0676$. CCDC 193519.

See <http://www.rsc.org/suppdata/cc/b2/b208872j/> for crystallographic data in CIF or other electronic format.

- e.g.* H. Köhler, A. Kolbe and G. Lux, *Z. Anorg. Allg. Chem.*, 1977, **428**, 103; J. L. Manson and J. S. Miller, *Inorg. Chem.*, 1999, **38**, 2552.
- Y. M. Chow and D. Britton, *Acta Cryst. Sect. B*, 1975, **31**, 1937.
- (a) S. W. Kaiser, Thesis, University of Michigan, 1975, 25; (b) P. Kircher, G. Huttner, K. Heinze, B. Schiemenz, L. Zsolnai, M. Büchner and A. Driess, *Eur. J. Inorg. Chem.*, 1998, 703.
- A. S. Abushamleh and H. A. Goodwin, *Aust. J. Chem.*, 1979, **32**, 513.
- J. L. Manson, C. R. Kmety, Q. Huang, J. W. Lynn, G. M. Bendele, S. Pagola, P. W. Stephens, L. Liable-Sands, A. L. Rheingold, A. J. Epstein and J. S. Miller, *Chem. Mater.*, 1998, **10**, 2552.
- J. Mrozinski, M. Hvastijová and J. Kohout, *Polyhedron*, 1992, **11**, 2867.
- S. R. Marshall, A. L. Rheingold, L. N. Dawe, W. W. Shum, C. Kitamura and J. S. Miller, *Inorg. Chem.*, 2002, **41**, 3599.
- D. Britton and Y.-M. Chow, *Acta Crystallogr., Sect B*, 1977, **33**, 697.
- J. Telsner and R. S. Drago, *Inorg. Chem.*, 1985, **24**, 4765.
- A. Adrait, L. Jacquamet, L. Le Pape, A. Gonzalez de Peredo, D. Aberdam, J.-L. Hazemann, J.-M. Latour and I. Michaud-Soret, *Biochemistry*, 1999, **38**, 6248.